Journal of Solid State Chemistry **147,** 291–295 (1999)
Article ID jssc.1999.8273, available online at http://www.idealibrary.com on IDEAL®

Crystal Structure and Magnetic Properties of B-Site Ordered Perovskite-type Oxides $A_2CuB'O_6$ (A = Ba, Sr; B' = W, Te)

Daisuke Iwanaga, Yoshiyuki Inaguma, and Mitsuru Itoh[1]

Materials and Structures Laboratory, Tokyo Institute of Technology, 4259 Nagatsuta, Midori-ku, Yokohama 226, Japan

Received November 4, 1998; in revised form March 9, 1999; accepted March 10, 1999

Four cuprate perovskites with the general formula $A_2CuB'O_6$ (A = Ba, Sr; B' = W, Te) were synthesized and the structural and the magnetic properties were investigated. Among four samples, perovskite Ba_2CuTeO_6 was formed only under high pressure. All the samples were tetragonally distorted B-site ordered perovskite-type oxides with *I*4/*m* symmetry. The CuO_6 octahedra is elongated by the Jahn–Teller effect of Cu^{2+} ion and CuO_6 and WO_6 (or TeO_6) octahedra rotates about the [001] direction. These compounds show two-dimensional antiferromagnetic behavior, because of the superexchange interaction between Cu^{2+} ions via an array of nonmagnetic ions, O–W–O (or O–Te–O) in the *ab*-plane perpendicular to the *c*-axis. The detailed analysis of the crystal structure made clear that the strength of the superexchange interaction depends more on the bond angle Cu–O–W (or Cu–O–Te) than the distance between Cu^{2+} ions in the *ab*-plane.

Key Words: **perovskite; superexchange interaction; Jahn–Teller effect; cuprate.**

INTRODUCTION

Oxides with general formula ABO_3 easily adopt the perovskite-type structure when A is a large ion and B is a relatively small metal ion. The six oxygens to which a B-site ion is coordinated construct octahedra. The octahedra share their corners forming a three-dimension structure. A ions occupy the open spaces in the three-dimensional network of oxygen octahedra. By a suitable combination of A and B ions, various kinds of perovskite oxides have been prepared. Besides simple combinations such as $A^+B^{5+}O_3$, $A^{2+}B^{4+}O_3$, or $A^{3+}B^{3+}O_3$, there are complex perovskite-type oxides with several B-site ions such as $A^{2+}(B^{3+}_{0.5}B'^{3+}_{0.5})O_3$, $A^{2+}(B^{2+}_{1/3}B'^{5+}_{2/3})O_3$.

Much research has been carried out with more than 1000 complex perovskite-type oxides having stoichiometries $A_2BB'O_6$, $A_3B_2B'O_9$, or $A_4B_3B'O_{12}$ (1–9). These oxides can be broadly classified into two types, B-site ordered and disorderd perovskites. Generally, there is a tendency to take a random sequence when the difference in the valences or ionic radii of two kinds of metal ion in B-sites is small.

When the complex perovskite-type oxides include transition metal ions in B-sites, the magnetic properties are strongly influenced by the ordering of B-site ions. For example, in B-site disordered perovskite-type oxides, $Sr_2FeRùO_6$ and $BaLaNiBiO_6$ (10–12), a spin glass behavior was observed at low temperatures. On the other hand, B-site ordered Sr_2FeMoO_6 exhibited ferrimagnetism (13).

B-site ordered perovskite-type oxides in which one B-site ion is magnetic and the other is nonmagnetic have been extensively studied by Blasse (14). Cubic Sr_2NiWO_6 is an example of this type of oxide. Here, Ni^{2+} is a magnetic ion having eight 3*d* electrons, while W^{6+} ion is a nonmagnetic one with a $5d^0$ electronic configuration. The Ni and W ions occupy B-sites alternatly, so that a nonmagnetic ion array, O–W–O, exists between Ni ions. Although the distance between Ni ions is large in Sr_2NiWO_6, superexchange interaction occurs via an array of nonmagnetic ions and antiferromagnetic behavior has been observed. This long range superexchange interaction is very weak compared with the interaction via only oxygen ions. As a result, the Neel temperature of Sr_2NiWO_6 is 54 K, while that of NiO is 523 K.

The ordered cuprate perovskites Ba_2CuWO_6 and Sr_2CuWO_6 are tetragonally distorted by the cooperative Jahn–Teller effect (15). In reports of Blasse, Ba_2CuWO_6 and Sr_2CuWO_6 showed different magnetic behavior at low temperatures compared to other B-site ordered perovskite-type oxides such as Sr_2NiWO_6. For these cuprate compounds, a sharp maximum in the temperature dependence of susceptibility corresponding to the Neel temperature was not observed. The temperature dependence of magnetic susceptibility showed a broad maximum and a sudden increase at low temperature. Blasse gave a qualitative explanation for this behavior as follows. Since the Cu^{2+} ion has electron configuration $t_{2g}^6e_g^3$ and CuO_6 octahedra are elongated

With deep regret we have learned of the sudden death of great scientist Dr. Jean Rouxel.

[1]To whom correspondence should be addressed.

0022-4596/99 $30.00

along the *c*-axis by a Jahn–Teller effect, the e_g orbital is split into d_{z^2} and $d_{x^2-y^2}$ orbitals. The d_{z^2} orbital is completely filled, whereas the $d_{x^2-y^2}$ orbital is half filled. The anomalous magnetic behavior depends on the 180° and 90° long range superexchange interactions between unpaired electrons in the *ab*-plane (14).

In this study, these two compounds were synthesized and the structure and magnetic properties were re-elucidated. Furthermore, in order to understand the influence of nonmagnetic B-site ions, the properties of Sr_2CuTeO_6 and Ba_2CuTeO_6 where the Te^{6+} ion has a $4d^{10}5s^05p^0$ electronic configuration were also investigated. The results for the samples are summarized and the relationship between the structure and magnetic properties was derived.

EXPERIMENTAL

Polycrystalline samples were prepared by a solid state reaction method. The starting materials, $BaCO_3$, $SrCO_3$, CuO, WO_3, and TeO_2, were weighed according to the stoichiometric cation composition dictated by the formulae of the final products and were mixed using ethanol as a medium in an agate mortor. The TeO_2 was added in 5 mol% excess, due to its high volatility. The weighed materials were mixed with ethanol in an agate mortor and fired in air. All samples were pressed into pellets and subjected to the following heat treatment. The Ba_2CuWO_6 and Sr_2CuWO_6 phases were prepared by firing at 1173 K for 12 h twice with an intermediate grinding and at 1273 K for 12 h, respectively. For Sr_2CuWO_6, sudden heating and quenching was necessary to avoid the formation of the impurity, $SrWO_4$. Sr_2CuTeO_6, and Ba_2CuTeO_6 were synthesized by firing at 1173 K for 12 h and at 1373 K for 12 h. Single phase samples with perovskite-type structures were obtained for all compositions except Ba_2CuTeO_6. The Ba_2CuTeO_6 phase was formed in a 4*H*-type hexagonal structure where some of the oxygen octahedra shared a face with one another (16). In order to obtain the perovskite-type Ba_2CuTeO_6, hexagonal-type Ba_2CuTeO_6 was heated at 1173 K for 10 min under 5 GPa by using a cubic anvil-type of high pressure equipment.

For phase identification and structure analysis, the powder X-ray diffraction data were recorded at room temperature using a MAC Science MXP18HF X-ray diffractometer with a graphite monochromatized Cu$K\alpha$ radiation ($\lambda = 1.54050$ Å). For Ba_2CuWO_6, neutron powder diffraction data only at 10 K and room temperature were collected on an HRPD angle-dispersive-type diffractometer at the JRR-3 reactor at the Japan Atomic Energy Research Institute. X-ray powder diffraction data were analyzed by the Rietveld method with RIETAN (17). The magnetic susceptibilities were measured in the temperature range 5–300 K using a SQUID magnetometer (Quantum Design MPMS-2) and in the range of 300–800 K using a Faraday magnetic balance (Shimadzu MB-2).

RESULTS AND DISCUSSION

Crystal Structure

All samples were confirmed to be single phases as determined by X-ray diffraction with a tetragonally distorted perovskite-type structure. As an example, the X-ray diffraction data for Ba_2CuWO_6 with observed and calculated patterns, differences, and the peak positions are shown in Fig. 1. The results of Rietveld analysis showed better *R*-factors, when the space group $I4/m$ (International Tables A, No. 87) was used. Structure parameters, interactomic distances, and *R* factors obtained from the Rietveld analysis are summarized in Table 1. For all samples, the tetragonality ratio c/a is between 1.093 and 1.102. The Rietveld analysis using neutron powder diffraction data for Ba_2CuWO_6 showed nearly the same result as that of XRD. The details will be reported in the future.

From the Rietveld analysis, Cu and W (or Te) were found to occupy alternate B-sites. Furthermore, CuO_6 octahedra are elongated along the *c*-axis. The dstances between Cu and O in the *ab*-plane and parallel to the *c*-axis are about 0.19 and 0.21 nm, respectively. On the other hand, WO_6 (or TeO_6) octahedra are compressed along the *c*-axis. Thus the tetragonal distortion can be ascribed to the cooperative Jahn–Teller effect of Cu^{2+} ions. CuO_6 and WO_6 (or TeO_6) octahedra rotate slightly around the [0 0 1] direction.

The lattice parameters for the Ba samples are larger than those for the Sr samples, because of the difference in the ionic radii of Ba Sr (Ba, 0.161 nm; Sr, 0.144 nm, when the coordination number is 12) (18). The compounds containing W and Te have nearly the same value for the lattice

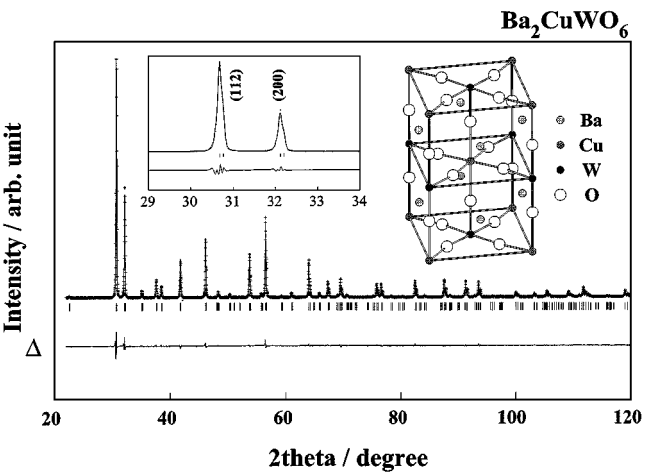

FIG. 1. Observed (solid line) and calculated (crosses) X-ray powder diffraction profiles of Ba_2CuWO_6. Δ indicates the difference between the observed and calculated data. The small vertical lines mark the positions of various reflections.

TABLE 1
Crystal Structure Data for $A_2CuB'O_6$ (A = Ba, Sr; B' = W, Te)[a]

	Ba_2CuWO_6	Sr_2CuWO_6	Sr_2CuTeO_6	Ba_2CuTeO_6
a (nm)	0.55642(1)	0.54290(1)	0.54308(1)	0.55903(1)
c (nm)	0.86363(4)	0.84155(2)	0.84664(3)	0.86426(3)
c ($\sqrt{2}a$)	1.097	1.096	1.102	1.093
V (nm^3)	0.2674	0.2480	0.2497	0.2701
O(1)(z)	0.280	0.276	0.280	0.281
O(2)(x)	0.272	0.289	0.297	0.263
y	0.238	0.213	0.206	0.244
Cu–O(ab) × 4(nm)	0.201(2)	0.195(3)	0.196(3)	0.201(3)
Cu–O(c) × 2(nm)	0.241(2)	0.232(3)	0.237(3)	0.243(3)
W, Te–O(ab)×4(nm)	0.193(2)	0.193(3)	0.197(3)	0.195(3)
W, Te–O(c) × 2(nm)	0.190(2)	0.188(3)	0.186(3)	0.190(3)
Ba, Sr–O × 4(nm)	0.283(3)	0.272(2)	0.272(1)	0.281(2)
Ba, Sr–O × 4(nm)	0.279(2)	0.266(2)	0.263(1)	0.289(1)
Ba, Sr–O × 4(nm)	0.301(3)	0.305(2)	0.310(1)	0.298(1)
Cu–O–W, Te(deg.)	172(3)	163(2)	159(1)	176(7)
R_{wp}	6.49	8.30	5.89	8.40
R_p	4.84	5.86	4.49	6.54
R_r	7.81	11.01	9.90	12.03
R_e	2.98	2.31	2.40	3.81
R_i	1.72	4.65	3.90	3.80
R_f	1.37	3.10	3.22	2.90

[a]The five atoms have the following positions: Ba or Sr (0, 1/2, 1/4), Cu (0, 0, 0), W or Te (0, 0, 1/2), O(1) (0, 0, z), O(2) (x, y, 0).

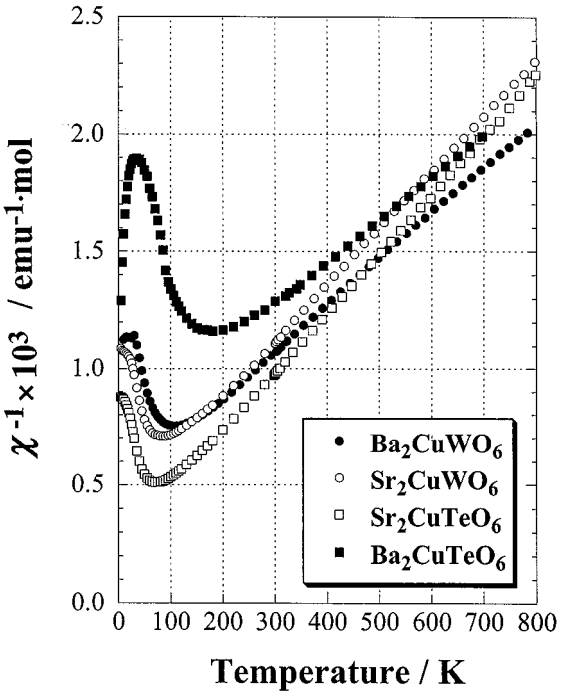

FIG. 2. Temperature dependence of magnetic susceptibility of Ba_2CuWO_6, Sr_2CuWO_6, Sr_2CuTeO_6, Ba_2CuTeO_6.

parameters. The angle between CuO_6 and WO_6 (or TeO_6) for Ba samples is larger than those for Sr samples. Though it is conceivable that the difference of electronic states in addition to the ionic radius between W^{6+} ($5d^06s^0$) and Te^{6+} ($4d^{10}5s^05p^0$) influences crystal structure, a marked difference was not ovserved in this study.

Magnetic Properties

The temperature dependence of the inverse of the magnetic susceptibilities for all of the samples are shown in Fig. 2. Above room temperature, all samples obeyed the Curie–Weiss law, $\chi = C/(T + \theta)$. The Curie constant and Weiss temperature obtained from the fitting to the Curie–Weiss law, the effective Bohr magneton, μ_{eff}, and the antiferromagnetic super-exchange interaction, J, of each sample are summarized in Table 2. Here, J was estimated by the high-temperature series expansion method (19) using the magnetic susceptibility data. The effective Bohr magneton, μ_{eff}, of the Cu^{2+} ion was calculated from the equation $\mu_B = 2\sqrt{S(S+1)}$ to be 1.73, where $S = 1/2$. The observed effective Bohr magneton values, μ_{eff}, of Sr_2CuWO_6 and Sr_2CuTeO_6 are nearly the same as the calculated value, showing that d-electons of the Cu^{2+} ion are nearly localized above room temperature. However, the effective Bohr magneton values of Ba_2CuWO_6 and Ba_2CuTeO_6 are a little larger than the calculated values. This implies that the orbital magnetic moments of electrons are not quenched. The values of the Weiss temperatures for the four samples are negative. This indicates that the magnetic interaction between Cu ions is an antiferromagnetic one. The antiferromagnetic interaction could arise from the superexchange interaction between Cu ions via an array of nonmagnetic ions, O–W–O or O–Te–O. The 5d and/or 6s orbital of the W^{6+} ion and the 5s and/or 5p orbital of the Te^{6+} ion must be used for the superexchange interaction.

The temperature dependences of magnetic susceptibility from 5 K to room temperature for Ba_2CuWO_6, Sr_2CuWO_6, Ba_2CuTeO_6, and Sr_2CuTeO_6 are shown in Fig. 2. Magnetic susceptibilities were measured under a magnetic field of 100 Oe after the sample was cooled in zero field and cooled in a 3 T field (Fig. 3). The magnetic behavior of these oxides

TABLE 2
Curie Constants (C), Effective Bohr Magneton (μ_{eff}), Weiss Temperature (θ), and J for $A_2CuB'O_6$ (A = Ba, Sr; B' = W, Te)

	Ba_2CuWO_6	Sr_2CuWO_6	Sr_2CuTeO_6	Ba_2CuTeO_6
C	0.51	0.42	0.40	0.54
μ_{eff}	1.93	1.75	1.71	1.98
θ (K)	−249	−168	−97	−400
J/k_B (K)	110	85	55	180

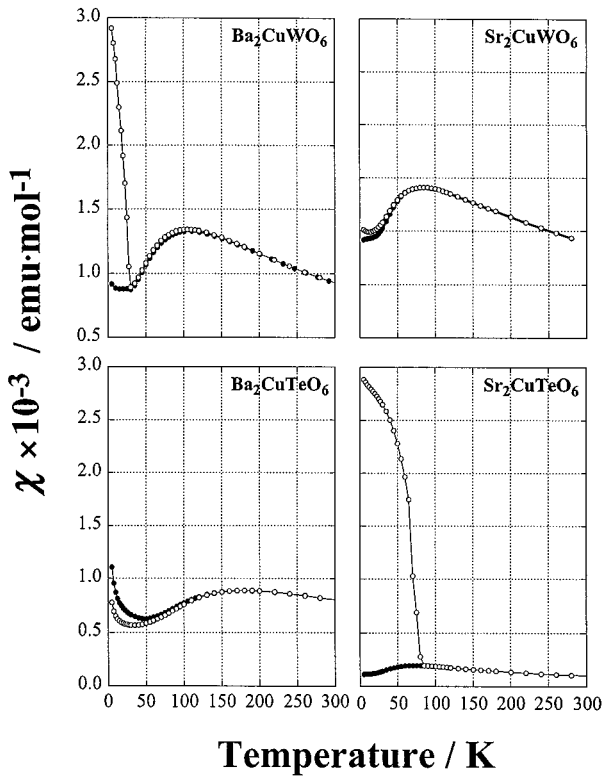

FIG. 3. Temperature dependence of magnetic susceptibility of $A_2CuB'O_6$ (A = Ba, Sr; B' = W, Te) at a measured applied field of 100 Oe. Open symbols represent zero field cooled data; closed symbols represent 3 tesla field cooled data.

are different from other B-site ordered perovskite-type oxides such as Sr_2NiWO_6, that show usual antiferromagnetic behavior. The temperature dependence of magnetic susceptibility for Sr_2NiWO_6 shows a clear maximum at the Neel temperature (14). However, in the case of Ba_2CuWO_6, a broad maximum in susceptibility at 110 K was observed. This indicates that three-dimensional antiferromagnetic ordering does not occur in Ba_2CuWO_6. This is also supported by the fact that the neutron diffraction pattern at 10 K is similar to the pattern at room temperature with no additional peaks observed (20). Such a behaviour is observed in low-dimensional magnetic materials. The electron configuration of the Cu^{2+} ion coordinated octahedrally by six oxygens is $t_{2g}^6 e_g^3$. As mentioned above, since the CuO_6 octahedra are elongated along the c-axis due to the Jahn–Teller effect, e_g orbitals split into two orbitals, $d_{x^2-y^2}$ and d_{z^2}. Two of the three electrons in the e_g orbital fill the low energy orbital (d_{z^2}) and the remaining one electron occupies the high energy orbital ($d_{x^2-y^2}$). Since the d_{z^2} orbital is fully occupied with two electrons, a 180° superexchange interaction does not occur along the c-axis direction. On the other hand, an antiferromagnetic 180° superexchange interaction betweeen Cu ions via an array of nonmagnetic ions exists in the ab-plane since the $d_{x^2-y^2}$ orbital is half filled. In addition, a 90° superexchange interaction between Cu ions is expected to be weak because the $d_{x^2-y^2}$ orbitals are orthogonal to each other. Hence, Ba_2CuWO_6 can be thought of as a two-dimensional antiferromagnetic material.

As Blasse observed in Ba_2CuWO_6 and Sr_2CuWO_6 (14), the rise of magnetic susceptibility was observed below 25 K, though it is very small. Furthermore, the rise depends on the magnetic field while cooling, though the magnetic susceptibility above 25 K is independent of the magnetic field. This phenomenon suggests the existence of weak ferromagnetic ordering below 25 K. When magnetic field dependence of magnetization was measured, a small hysteresis loop was observed. There was no difference between zero field cooled and 3 T field cooled results.

Other samples showed similar behavior as that for Ba_2CuWO_6. However, the temperatures corresponding to the anomaly in magnetic susceptibility are different among these samples. The J is a parameter that shows the strength of the antiferromagnetic superexchange interaction. Since the absolute value of the Weiss temperature, θ, and μ_{eff} for each sample shows almost the same tendency, θ and μ_{eff} are good parameters to evaluate the strength of the superexchange interaction. The strength of the superexchange interaction is known to depend on the bond length and the bond angle between magnetic ions (21). The relationship between the bond length (Cu–O) in the ab-plane, the bond angle

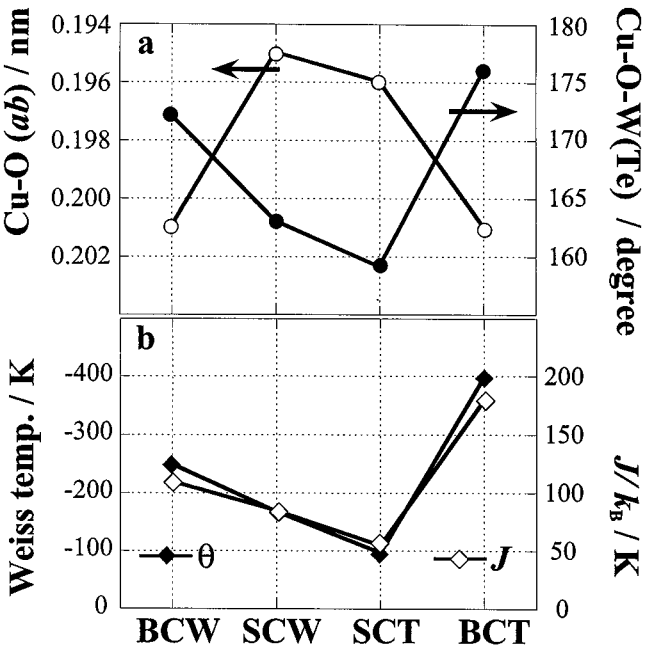

FIG. 4. The relation between the crystal structure and magnetic properties of Ba_2CuWO_6 (BCW), Sr_2CuWO_6 (SCW), Sr_2CuTeO_6 (SCT), and Ba_2CuTeO_6 (BCT). (a) The bond length, Cu–O in the ab-plane and the bond angles, Cu–O–W or Cu–O–Te. (b) Weiss temperature, θ, and the antiferromagnetic superexchange interaction, J, obtained from the high temperature expansion approximation.

(Cu–O–W or Cu–O–Te), and the Weiss temperature are shown in Fig. 4. As is clear from Fig. 4, the strength of the superexchange interaction depends on the bond angle more effectively than the bond length in this system.

CONCLUSIONS

B-site ordered perovskite-type oxides, Ba_2CuWO_6, Sr_2CuWO_6, Sr_2CuTeO_6, and Ba_2CuTeO_6, are found to show two-dimensional antiferromagnetic behavior. The two-dimensional antiferromagnetic interaction originates from the Jahn–Teller effect of Cu^{2+} ions. Furthermore, the rise of magnetic susceptibility at low temperatures and its deviation when the sample was cooled under magnetic field are observed for all samples. It is found that the strength of the superexchange interaction depends mainly on the bond angle, Cu–O–W (or Cu–O–Te), in these cuprate systems.

ACKNOWLEDGMENTS

Part of this work was financially supported by JSPS Research for the Future program, "Atomic-Scale Surface and Interface Dynamics" and a Grant-in-aid for scientific research from the Ministry of Education, Science, and Culture, Japan.

REFERENCES

1. G. Blasse, *J. Inorg. Nucl. Chem.* **27,** 993 (1965).
2. G. Kapyshev, V. V. Ivanova, and Yu. N. Venevtsev, *Soviet Phys. Dokl.* **11,** 195 (1966).
3. G. Blasse, *Phys. Proc. Kon. Ned. Aka. Wet*. **67,** 312 (1964).
4. F. Galasso, and W. Darby, *J. Phys. Chem.* **66,** 131 (1962).
5. E. J. Fresia, L. Katz, and R. Ward, *J. Am. Chem. Soc*. **81,** 4783 (1959).
6. F. Galasso, L. Katz, and R. Ward, *J. Am. Chem. Soc*. **81,** 820 (1959).
7. J. A. Alanso, E. Mzayek, and I. Rasines, *Mat. Res. Bull.* **22,** 69 (1987).
8. M. F. Kupriyanov and E. G. Fesenko, *Soviet Phys. Crystallogr.* **7,** 358 (1962).
9. Galasso, Francis. S., "Perovskites and High T_c Superconductors," Gordon & Breach, New York, 1990.
10. P. D. Battle, T. C. Gibb, A. J. Herod, S. H. Kim, and P. H. Hunns, *J. Mater. Chem.* **5,** 75 (1995).
11. P. D. Battle, T. C. Gibb, A. J. Herod, and J. P. Hodges, *J. Mater. Chem.* **5,** 865 (1995).
12. S. H. Kim, and P. D. Battle, *J. Solid State Chem.* **114,** 174 (1995).
13. S. Nakayama, T. Nakagawa, and S. Nomura, *J. Phys. Soc. Jpn.* **24,** 19 (1968).
14. G. Blasse. *Philips Res. Rep.* **20,** 327 (1965).
15. Bokhimi, *Powder Diffraction* **7,** No. 4, 228 (1992).
16. P. Kohl and D. Reinen, *Z. Anorg. Allg. Chemie.* **409,** 257 (1974).
17. F. Izumi, H. Murata, and N. Watanabe, *J. Appl. Crystallogr.* **20,** 411 (1987).
18. R. D. Shannon, *Acta Cryst. A* **32,** 751 (1976).
19. G. R. Rushbrooks, G. A. Baker, Jr., and P. J. Wood, *in* "Phase Transitions and Critical Phenomena" (C. Domb and M. S. Green, Eds.), Vol. 3, Chap. 5. Academic Press, New York, 1974.
20. Y. Inaguma, D. Iwanaga, M. Itoh, K. Aizawa, Y. Shimojo, and Y. Morii, "Progress Report on Neutron Scattering Research," JAERI-Review 97-012, p. 11 (1997).
21. J. B. Goodenough, "Magnetism and the Chemical Bond," Interscience, New York, 1963.